supplemented with 5% horse serum (Invitrogen), 100 units/ml penicillin and 100 μg/ml streptomycin]. Six days following induction of differentiation, myotubes were used for $[Ca^{2+}]_i$ imaging or a Mn^{2+} quenching assay.

Transfected HEK293 cells were lifted using trypsin and seeded onto poly-L-lysine-coated glass cover slips at 8 h post-transfection. Note that trypsinized cells were cultured in low-Ca^{2+} D-MEM (Life Technologies), which was supplemented with 10% FBS, 2 mM glutamine, 30 units/ml penicillin, 30 μg/ml streptomycin, 0.2 mM $CaCl_2$ and 10 μM La^{3+}, to prevent Ca^{2+} overload-induced cell death (31). $[Ca^{2+}]_i$ imaging was performed at 24–36 h after transfection.

Measurement of changes in $[Ca^{2+}]_i$

HEK293 cells on cover slips were loaded with Fura-2 by incubation in low-Ca^{2+} D-MEM containing 5 μM Fura-2/AM (Dojindo Laboratories) at 37°C for 40 min, and washed with imaging solution (2Ca). The cover slips were then placed in a perfusion chamber mounted on the stage of a microscope (Axio-observer Z1; Carl Zeiss). Transfected cells were identified by detection of fluorescence from pDsRed-Monomer. Fura-2 fluorescence images of the cells were recorded and analyzed with Physiology software (Carl Zeiss). The 340/380 nm ratios of images were recorded at 10 s intervals. The compositions of $[Ca^{2+}]_i$ imaging solutions are listed in Supplementary Material, Table S6. Fura-2/AM was loaded into skeletal myotubes on cover slips in the same manner used for HEK293 cells but in nominally Ca^{2+}-free HEPES-buffered saline (HBS) (Supplementary Material, Table S6). The cover slips were then placed in a perfusion chamber mounted on the stage of the microscope (IX70; Olympus). Fura-2 fluorescence images of the myotubes were recorded and analyzed with MetaMorph Imaging Software (Molecular Devices). The images were recorded at 20 s intervals. Compositions of $[Ca^{2+}]_i$ imaging solutions are listed in Supplementary Material, Table S6. For measurement of the resting $[Ca^{2+}]_i$, Fura-2/AM was loaded to myotubes at 0Ca and 2Ca, respectively, and $[Ca^{2+}]_i$ imaging was performed. The resting $[Ca^{2+}]_i$ was calculated as previously reported (45).

Mn^{2+} quenching assay

Extracellular Mn^{2+} entry was measured through monitoring the decline in the fluorescence intensity of Fura-2 at an isosbestic excitation wavelength of 360 nm and recording the emitted fluorescence at 510 nm (46) by using the same system as used for the $[Ca^{2+}]_i$ measurement. The compositions of nominally Ca^{2+}-free HBS and 0.1 mM $MnCl_2$ solutions are listed in Supplementary Material, Table S6.

Statistical analysis

Graphics were prepared and statistical analyses were performed with GraphPad Prism (GraphPad Software). Data are presented as mean ± SEM. All data were analyzed using unpaired *t*-tests in comparisons between two samples and ANOVA in comparisons among three samples.

WEB RESOURCES

Online Mendelian Inheritance in Man (OMIM), http://www.omim.org/.
dbSNP, http://www.ncbi.nlm.nih.gov/projects/SNP/.
1000 Genomes Project, http://www.1000genomes.org/.
NHLBI Exome Sequencing Project (ESP) Exome Variant Server, http://eversusgs.washington.edu/EVS/.
HGVD, http://www.genome.med.kyoto-u.ac.jp/SnpDB/.
MutationTaster, http://www.mutationtaster.org/.
SIFT, http://sift.jcvi.org.
PolyPhen-2, http://genetics.bwh.harvard.edu/pph2/.
MMDB, http://www.ncbi.nlm.nih.gov/Structure/MMDB/mmdb.shtml.
BWA, http://bio-bwa.sourceforge.net/.
Picard, http://picard.sourceforge.net/.
GATK, http://www.broadinstitute.org/gatk/.
ANNOVAR, http://www.openbioinformatics.org/annovar/.

SUPPLEMENTARY MATERIAL

Supplementary Material is available at *HMG* online.

ACKNOWLEDGEMENTS

We thank T. Uchiumi, K. Goto, A. Kaminaga, K. Tatezawa and M. Ogawa for technical assistance. The antibodies XA7B6 for anti-RYR1 and IIID5E1 for anti-DHPR developed by K.P. Campbell were obtained from the Developmental Studies Hybridoma Bank developed under auspices of the NICHD and maintained by the University of Iowa, Department of Biology, Iowa City, IA52242.

Conflict of Interest statement. None declared.

FUNDING

This work was supported by an Intramural Research Grant (26-8, 25-5, 23-4) for Neurological and Psychiatric Disorders of the NCNP (to S.N., Y.H., I.N.) and by a Research on Applying Health Technology grant (H23-JITSUYOUKA(NANBYOU)-IPPAN-008, H26-ITAKU(NAN)-IPPAN-081) from the Ministry of Health, Labour and Welfare (to I.N.).

REFERENCES

1. Shoback, D. (2008) Clinical practice. Hypoparathyroidism. *New Eng. J. Med.*, **359**, 391–403.
2. Rossi, A.E. and Dirksen, R.T. (2006) Sarcoplasmic reticulum: the dynamic calcium governor of muscle. *Muscle Nerve*, **33**, 715–731.
3. Vig, M., Peinelt, C., Beck, A., Koomoa, D.L., Rabah, D., Koblan-Huberson, M., Kraft, S., Turner, H., Fleig, A., Penner, R. and Kinet, J.P. (2006) CRACM1 is a plasma membrane protein essential for store-operated Ca^{2+} entry. *Science*, **312**, 1220–1223.
4. Yeromin, A.V., Zhang, S.L., Jiang, W., Yu, Y., Safrina, O. and Cahalan, M.D. (2006) Molecular identification of the CRAC channel by altered ion selectivity in a mutant of Orai. *Nature*, **443**, 226–229.
5. Liou, J., Kim, M.L., Heo, W.D., Jones, J.T., Myers, J.W., Ferrell, J.E. and Meyer, T. (2005) STIM is a Ca^{2+} sensor essential for Ca^{2+}-store-depletion-triggered Ca^{2+} influx. *Curr. Biol.*, **15**, 1235–1241.
6. Roos, J., DiGregorio, P.J., Yeromin, A.V., Ohlsen, K., Lioudyno, M., Zhang, S., Safrina, O., Kozak, J.A., Wagner, S.L., Cahalan, M.D. *et al.* (2005) STIM1, an essential and conserved component of store-operated Ca^{2+} channel function. *J. Cell Biol.*, **169**, 435–445.
7. Zhang, S.L., Yu, Y., Roos, J., Kozak, J.A., Deerinck, T.J., Ellisman, M.H., Stauderman, K.A. and Cahalan, M.D. (2005) STIM1 is a Ca^{2+} sensor that

activates CRAC channels and migrates from the Ca^{2+} store to the plasma membrane. *Nature*, **437**, 902–905.
8. Prakriya, M., Feske, S., Gwack, Y., Srikanth, S., Rao, A. and Hogan, P.G. (2006) Orai1 is an essential pore subunit of the CRAC channel. *Nature*, **443**, 230–233.
9. Stathopulos, P.B., Li, G.-Y., Plevin, M.J., Ames, J.B. and Ikura, M. (2006) Stored Ca^{2+} depletion-induced oligomerization of stromal interaction molecule 1 (STIM1) via the EF-SAM region: an initiation mechanism for capacitive Ca^{2+} entry. *J. Biol. Chem.*, **281**, 35855–35862.
10. Luik, R.M., Wu, M.M., Buchanan, J. and Lewis, R.S. (2006) The elementary unit of store-operated Ca^{2+} entry: local activation of CRAC channels by STIM1 at ER-plasma membrane junctions. *J. Cell Biol.*, **174**, 815–825.
11. Park, C.Y., Hoover, P.J., Mullins, F.M., Bachhawat, P., Covington, E.D., Raunser, S., Walz, T., Garcia, K.C., Dolmetsch, R.E. and Lewis, R.S. (2009) STIM1 clusters and activates CRAC channels via direct binding of a cytosolic domain to Orai1. *Cell*, **13**, 876–890.
12. Wu, M.M., Buchanan, J., Luik, R.M. and Lewis, R.S. (2006) Ca^{2+} store depletion causes STIM1 to accumulate in ER regions closely associated with the plasma membrane. *J. Cell Biol.*, **174**, 803–813.
13. Feske, S., Gwack, Y., Prakriya, M., Srikanth, S., Puppel, S.-H., Tanasa, B., Hogan, P.G., Lewis, R.S., Daly, M. and Rao, A. (2006) A mutation in Orai1 causes immune deficiency by abrogating CRAC channel function. *Nature*, **441**, 179–185.
14. McCarl, C.A., Picard, C., Khalil, S., Kawasaki, T., Röther, J., Papolos, A., Kutok, J., Hivroz, C., Ledeist, F., Plogmann, K., Ehl, S. *et al.* (2009) ORAI1 deficiency and lack of store-operated Ca^{2+} entry cause immunodeficiency, myopathy, and ectodermal dysplasia. *J. Allergy Clin. Immunol.*, **124**, 1311–1318.
15. Picard, C., McCarl, C.-A., Papolos, A., Khalil, S., Lüthy, K., Hivroz, C., LeDeist, F., Rieux-Laucat, F., Rechavi, G., Rao, A. *et al.* (2009) STIM1 mutation associated with a syndrome of immunodeficiency and autoimmunity. *New Eng. J. Med.*, **360**, 1971–1980.
16. Böhm, J., Chevessier, F., Maues De Paula, A., Koch, C., Attarian, S., Feger, C., Hantaï, D., Laforêt, P., Ghorab, K., Vallat, J.M. *et al.* (2013) Constitutive activation of the calcium sensor STIM1 causes tubular-aggregate myopathy. *Am. J. Hum. Genet.*, **92**, 271–278.
17. Jain, D., Sharma, M.C., Sarkar, C., Suri, V., Sharma, S.K., Singh, S. and Das, T.K. (2008) Tubular aggregate myopathy: a rare form of myopathy. *J. Clin. Neurosci.*, **15**, 1222–1226.
18. Nesin, V., Wiley, G., Kousi, M., Ong, E.C., Lehmann, T., Nicholl, D.J., Suri, M., Shahrizaila, N., Katsanis, N., Gaffney, P.M., Wierenga, K.J. and Tsiokas, L. (2014) Activating mutations in STIM1 and ORAI1 cause overlapping syndromes of tubular myopathy and congenital miosis. *Proc. Natl Acad. Sci. USA*, **11**, 4197–4202.
19. Misceo, D., Holmgren, A., Louch, W.E., Holme, P.A., Mizobuchi, M., Morales, R.J., De Paula, A.M., Stray-Pedersen, A., Lyle, R., Dalhus, B. *et al.* (2014) A dominant STIM1 mutation causes Stormorken syndrome. *Hum. Mutat.*, **35**, 556–564.
20. Chevessier, F., Marty, I., Paturneau-Jouas, M., Hantaï, D. and Verdière-Sahuqué, M. (2004) Tubular aggregates are from whole sarcoplasmic reticulum origin: alterations in calcium binding protein expression in mouse skeletal muscle during aging. *Neuromus. Disord.*, **14**, 208–216.
21. Chevessier, F., Bauché-Godard, S., Leroy, J.-P., Koenig, J., Paturneau-Jouas, M., Eymard, B., Hantaï, D. and Verdière-Sahuqué, M. (2005) The origin of tubular aggregates in human myopathies. *J. Pathol.*, **207**, 313–323.
22. Salviati, G., Pierobon-Bormioli, S., Betto, R., Damiani, E., Angelini, C., Ringel, S.P., Salvatori, S. and Margreth, A. (1985) Tubular aggregates: sarcoplasmic reticulum origin, calcium storage ability, and functional implications. *Muscle Nerve*, **8**, 299–306.
23. Schiaffino, S. (2012) Tubular aggregates in skeletal muscle: just a special type of protein aggregates? *Neuromuscul. Disord.*, **22**, 199–207.
24. Hou, X., Pedi, L., Diver, M.M. and Long, S.B. (2012) Crystal structure of the calcium release-activated calcium channel Orai. *Science*, **338**, 1308–1313.
25. Prakriya, M. and Lewis, R.S. (2001) Potentiation and inhibition of Ca^{2+} release-activated Ca^{2+} channels by 2-aminoethyldiphenyl borate (2-APB) occurs independently of IP(3) receptors. *J. Physiol.*, **536**, 3–19.
26. Ishikawa, J., Ohga, K., Yoshino, T., Takezawa, R., Ichikawa, A., Kubota, H. and Yamada, T. (2003) A pyrazole derivative, YM-58483, potently inhibits store-operated sustained Ca^{2+} influx and IL-2 production in T lymphocytes. *J. Immunol.*, **170**, 4441–4449.
27. Kilch, T., Alansary, D., Peglow, M., Dörr, K., Rychkov, G., Rieger, H., Peinelt, C. and Niemeyer, B.A. (2013) Mutations of the Ca^{2+}-sensing stromal interaction molecule STIM1 regulate Ca^{2+} influx by altered oligomerization of STIM1 and by destabilization of the Ca^{2+} channel Orai1. *J. Biol. Chem.*, **288**, 1653–1664.
28. Gwack, Y., Srikanth, S., Feske, S., Cruz-Guilloty, F., Oh-hora, M., Neems, D.S., Hogan, P.G. and Rao, A. (2007) Biochemical and functional characterization of Orai proteins. *J. Biol. Chem.*, **282**, 16232–16243.
29. Zhou, Y., Ramachandran, S., Oh-Hora, M., Rao, A. and Hogan, P.G. (2010) Pore architecture of the ORAI1 store-operated calcium channel. *Proc. Natl Acad. Sci. USA*, **107**, 4896–4901.
30. Muik, M., Frischauf, I., Derler, I., Fahrner, M., Bergsmann, J., Eder, P., Schindl, R., Hesch, C., Polzinger, B., Fritsch, R. *et al.* (2008) Dynamic coupling of the putative coiled-coil domain of ORAI1 with STIM1 mediates ORAI1 channel activation. *J. Biol. Chem.*, **283**, 8014–8022.
31. Zhang, S.L., Yeromin, A.V., Hu, J., Amcheslavsky, A., Zheng, H. and Cahalan, M.D. (2011) Mutations in Orai1 transmembrane segment 1 cause STIM1-independent activation of Orai1 channels at glycine 98 and channel closure at arginine 91. *Proc. Natl Acad. Sci. USA*, **108**, 17838–17843.
32. McNally, B.A., Somasundaram, A., Yamashita, M. and Prakriya, M. (2012) Gated regulation of CRAC channel ion selectivity by STIM1. *Nature*, **482**, 241–245.
33. Zheng, H., Zhou, M.-H., Hu, C., Kuo, E., Peng, X., Hu, J., Kuo, L. and Zhang, S.L. (2013) Differential roles of the C and N termini of Orai1 protein in interacting with stromal interaction molecule 1 (STIM1) for Ca^{2+} release-activated Ca^{2+} (CRAC) channel activation. *J. Biol. Chem.*, **288**, 11263–11272.
34. Wei-Lapierre, L., Carrell, E.M., Boncompagni, S., Protasi, F. and Dirksen, R.T. (2013) Orai1-dependent calcium entry promotes skeletal muscle growth and limits fatigue. *Nat. Commun.*, **4**, 2805.
35. Senderek, J., Müller, J.S., Dusl, M., Strom, T.M., Guergueltcheva, V., Diepolder, I., Laval, S.H., Maxwell, S., Cossins, J., Krause, S. *et al.* (2011) Hexosamine biosynthetic pathway mutations cause neuromuscular transmission defect. *Am. J. Hum. Genet.*, **88**, 162–172.
36. Belaya, K., Finlayson, S., Slater, C.R., Cossins, J., Liu, W.W., Maxwell, S., McGowan, S.J., Maslau, S., Twigg, S.R., Walls, T.J. *et al.* (2012) Mutations in DPAGT1 cause a limb-girdle congenital myasthenic syndrome with tubular aggregates. *Am. J. Hum. Genet.*, **91**, 193–201.
37. Kiviluoto, S., Decuypere, J.P., De Smedt, H., Missiaen, L., Parys, J.B. and Bultynck, G. (2011) STIM1 as a key regulator for Ca^{2+} homeostasis in skeletal-muscle development and function. *Skelet. Muscle*, **1**, 16.
38. Kumar, R. and Thompson, J.R. (2011) The regulation of parathyroid hormone secretion and synthesis. *J. Am. Soc. Nephrol.*, **22**, 216–224.
39. Fukumoto, S., Namba, N., Ozono, K., Yamauchi, M., Sugimoto, T., Michigami, T., Tanaka, H., Inoue, D., Minagawa, M., Endo, I. and Matsumoto, T. (2008) Causes and differential diagnosis of hypocalcemia—recommendation proposed by expert panel supported by ministry of health, labour and welfare, Japan. *Endocr. J.*, **55**, 787–794.
40. Malicdan, M.C., Noguchi, S. and Nishino, I. (2009) Monitoring autophagy in muscle diseases. *Methods Enzymol.*, **453**, 379–396.
41. Li, H. and Durbin, R. (2009) Fast and accurate short read alignment with Burrows-Wheeler transform. *Bioinformatics*, **25**, 1754–1760.
42. DePristo, M.A., Banks, E., Poplin, R., Garimella, K.V., Maguire, J.R., Hartl, C., Philippakis, A.A., Angel, G., Rivas, M.A., Hanna, M. *et al.* (2009) A framework for variation discovery and genotyping using next-generation DNA sequencing data. *Nat. Genet.*, **43**, 491–498.
43. Wang, K., Li, M. and Hakonarson, H. (2010) ANNOVAR: functional annotation of genetic variants from high-throughput sequencing data. *Nucleic Acids Res.*, **38**, e164.
44. Maniatis, T., Fritsch, E.F. and Sambrook, J. (1982) *Molecular Cloning: A Laboratory Manual*. Cold Spring Harbor Laboratory Press, Cold Spring Harbor, NY.
45. Ihara, Y., Urata, Y., Goto, S. and Kondo, T. (2006) Role of calreticulin in the sensitivity of myocardiac H9c2 cells to oxidative stress caused by hydrogen peroxide. *Am. J. Physiol. Cell Physiol.*, **290**, C208–C221.
46. Pan, Z., Zhao, X. and Brotto, M. (2012) Fluorescence-based measurement of store-operated calcium entry in live cells: from cultured cancer cell to skeletal muscle fiber. *J. Vis. Exp.*, **13**, e3415.

DAG1 mutations associated with asymptomatic hyperCKemia and hypoglycosylation of α-dystroglycan

Mingrui Dong, MD
Satoru Noguchi, PhD
Yukari Endo, MD
Yukiko K. Hayashi, MD, PhD
Shinobu Yoshida, MD, PhD
Ikuya Nonaka, MD, PhD
Ichizo Nishino, MD, PhD

Correspondence to Dr. Noguchi: noguchi@ncnp.go.jp

ABSTRACT

Objectives: To identify gene mutations in patients with dystroglycanopathy and prove pathogenicity of those mutations using an in vitro cell assay.

Methods: We performed whole-exome sequencing on 20 patients, who were previously diagnosed with dystroglycanopathy by immunohistochemistry and/or Western blot analysis. We also evaluated pathogenicity of identified mutations for phenotypic recovery in a *DAG1*-knockout haploid human cell line transfected with mutated DAG1 complementary DNA.

Results: Using exome sequencing, we identified compound heterozygous missense mutations in *DAG1* in a patient with asymptomatic hyperCKemia and pathologically mild muscular dystrophy. Both mutations were in the N-terminal region of α-dystroglycan and affected its glycosylation. Mutated DAG1 complementary DNAs failed to rescue the phenotype in *DAG1*-knockout cells, suggesting that these are pathogenic mutations.

Conclusion: Novel mutations in *DAG1* are associated with asymptomatic hyperCKemia with hypoglycosylation of α-dystroglycan. The combination of exome sequencing and a phenotype-rescue experiment on a gene-knockout haploid cell line represents a powerful tool for evaluation of these pathogenic mutations. **Neurology® 2015;84:273-279**

GLOSSARY

cDNA = complementary DNA; ***DAG1*** = dystroglycan 1 (dystrophin-associated glycoprotein 1); **KO** = knockout; **WES** = whole-exome sequencing.

Dystroglycan is a central component of the dystrophin–glycoprotein complex, which links the cytoskeleton and extracellular matrix through sarcolemma.[1,2] Dystroglycan has important roles in the development and maintenance of skeletal muscle, the CNS,[3] and other organs.[4–6] It is encoded by the *DAG1* gene. The synthesized polypeptide is posttranslationally cleaved into 2 subunits, namely, α- and β-dystroglycan; then the former is highly glycosylated.[7,8] α-Dystroglycan is composed of 3 distinct domains: the N-terminal region, the mucin-like domain, and the C-terminal domain, at which the mucin-like domain is highly glycosylated by *O*-linked mannosyl-oligosaccharides and binds to ligands such as laminin and agrin by its sugar chains.[9,10] Reports show that the N-terminal region is required for functional glycosylation of the mucin-like domain by LARGE, an intracellular enzyme-substrate recognition motif necessary for initiation of specific glycosylation.[8,11]

Defects in glycosylation of α-dystroglycan lead to a subgroup of muscular dystrophies and brain and eye malformations, termed dystroglycanopathies.[12] There is a broad spectrum of severity in these diseases, ranging from Walker-Warburg syndrome, muscle-eye-brain disease, and Fukuyama congenital muscular dystrophy to the milder form of limb-girdle muscular dystrophy, such as LGMD2I.[13,14] Recent advances in DNA sequencing techniques facilitated identification of new causative genes in dystroglycanopathies[15–18]; to date, 18 causative genes have been identified. Among them, *DAG1* mutations cause primary dystroglycanopathy in limb-girdle muscular dystrophy[19] and muscle-eye-brain disease.[20]

Supplemental data at Neurology.org

From the Department of Neuromuscular Research, National Institute of Neuroscience (M.D., S.N., Y.E., Y.K.H., I. Nonaka, I. Nishino) and Department of Clinical Development, Translational Medical Center (S.N., Y.E., Y.K.H., I. Nishino), NCNP, Tokyo, Japan; Department of Neurology (M.D.), China-Japan Friendship Hospital, Beijing, China; Department of Neurophysiology (Y.K.H.), Tokyo Medical University; and Department of Pediatrics (S.Y.), Omihachiman Community Medical Center, Shiga, Japan.

Go to Neurology.org for full disclosures. Funding information and disclosures deemed relevant by the authors, if any, are provided at the end of the article.

Herein, we report the case of a patient in whom dystroglycanopathy was caused by novel compound heterozygous missense mutations in *DAG1* identified by whole-exome sequencing (WES) and we prove the pathogenicity of the mutations.

METHODS Standard protocol approvals, registrations, and patient consents. The ethics committee of the National Center of Neurology and Psychiatry approved this study. All patients gave written informed consent before study participation.

Subjects. To identify the cause of α-dystroglycanopathy, we selected a cohort of 20 unrelated individuals who were diagnosed with α-dystroglycanopathy by negative reactivity with an antibody for glycoepitope of α-dystroglycan (VIA4-1; Millipore, Billerica, MA) on a muscle biopsy and/or decreased VIA4-1 immunoreactivity and laminin binding ability as shown by Western blotting.[21] We immunostained muscle with antibodies for β-dystroglycan (43DAG1; Leica, Wetzlar, Germany), dystrophin (NCL-DYS1, Leica), merosin (4H8-2; Alexis, Lausen, Switzerland), and β-sarcoglycan (5B1, Leica), and conducted Western blotting using the core antibody for α-dystroglycan peptide, GT20ADG. We confirmed that all study patients did not have 3-kb retrotransposal insertion at *FKTN*.

Whole-exome sequencing. WES was performed as reported previously.[22] Briefly, after genomic DNA isolation from muscle specimens or peripheral blood lymphocytes using standard techniques, we performed exon capture according to the manufacturer's instructions (SureSelect Human All Exon kit V4, 50 Mb; Agilent, Santa Clara, CA), followed by paired-end 100-base massively parallel sequencing on an Illumina HiSeq1000 (Illumina, Inc., San Diego, CA). Then, we mapped and aligned to the human genome chromosomal sequence using the Burrows-Wheeler Aligner. We removed duplicate reads using Picard for downstream analysis and conducted local realignments around indels and regions for low base quality scores using the Genome Analysis Toolkit for recalibration. We identified single-nucleotide variants and small indels using the Genome Analysis Toolkit Unified Genotyper (version 1.6) and filtered according to the Broad Institute's best-practice guidelines. We used ANNOVAR to annotate genetic variations. Data filtering included the following conditions: (1) mutation effect—splicing, start lost, exon deletion, frame shift, stop gained or lost, nonsynonymous codon change, codon insertion or deletion; (2) variation frequency less than 0.01 in HapMap and in 1000 Genomes Project database; and (3) inheritance mode—homozygous mutations, hemizygous mutation, or more than 2 mutations in the same genes. We used Sanger sequencing to confirm mutations.

Validation for the pathogenicity of identified mutations. To examine the pathogenicity of identified mutations, we analyzed functional recovery of dystroglycans in *DAG1*-knockout (KO) haploid human cell line (HAP1) cells using transfection of lentivirus vectors, pLVSIN-IRES-ZsGreen (Clontech, Mountain View, CA), harboring wild-type or mutated human DAG1 complementary DNA (cDNA). Jae et al.[23] established the *DAG1*-KO HAP1 cell as reported previously. For the glycosylation in α-dystroglycan assay, we cultured HAP1 cells on laminin-coated glass-bottom dishes. Five days after lentivirus infection, we incubated live cells with IIH6-C4 antibody against glycoepitope of α-dystroglycan (Millipore) in medium and then visualized the cells with Alexa Fluor 568-labeled anti-mouse immunoglobulin M secondary antibody. We observed the cultured cells using a fluorescent microscope (BZ-9000; Keyence, Itasca, IL) with Z-axis scanning throughout whole cells to acquire green fluorescent protein and α-dystroglycan images together (7 images with 1-μm intervals) for full-focus images. After staining with 43DAG1 antibody and GM130 antibody (Cell Signaling Technology, Beverly, MA), we observed localization of β-dystroglycan in formalin-fixed HAP1 cells.

Biotinylation of cell-surface proteins on HAP1 cells. We labeled living HAP1 cells with the membrane-impermeable biotin reagent, Sulfo-NHS-LC-Biotin, according to manufacturer's instructions (Thermo Scientific, Waltham, MA) and then subjected streptavidin-purified proteins to Western blotting using standard techniques. We detected β-dystroglycans with 43DAG1 antibody.

RESULTS Identification of *DAG1* mutation by WES. After analysis of a cohort of 20 unrelated patients with α-dystroglycanopathy, we identified one patient who harbored mutations in *DAG1* genes. WES analysis summary is presented in table e-1 on the *Neurology*® Web site at Neurology.org. We identified 7 genes with homozygous mutations, 18 genes with compound heterozygous mutations, and 8 genes with hemizygous mutations in this patient (data not shown). Among them, we identified compound heterozygous mutations, c.220G>A (rs189360006) and c.331G>A (rs117209107) in *DAG1*, which are predicted to lead to missense mutations, p.Val74Ile and p.Asp111Asn, respectively. We did not find any other genes involved in the glycosylation pathway in the patient. We confirmed the 2 mutations in *DAG1* by Sanger sequencing (figure 1A) and the compound heterozygosity by transcript analysis (data not shown). Residues at both mutated sites are located in the N-terminal region of α-dystroglycan and are highly conserved during evolution (figure 1, B and C). In silico analyses of mutation function demonstrated that p.Val74Ile and p.Asp111Asn, respectively, were predicted as damaging and tolerated by SIFT and probably damaging and benign in PolyPhen-2, and both mutations were predicted as disease-causing in MutationTaster. Other than *DAG1* mutations, the compound heterozygous missense alterations were found in *TTN* and *AHNAK* genes among muscle-related genes.

Clinical phenotype and histologic features of muscle biopsy. This is a 7-year-old boy coming from a nonconsanguineous marriage who has compound heterozygous mutations in *DAG1*. He was born normally (length at birth, 51.5 cm; birth weight, 3,672 g) and demonstrated normal development milestones. At the age of 4 years and 7 months, he was 98 cm tall, weighed 17 kg, and had a head circumference of 50.8 cm. When he was 4 years

Figure 1 Compound heterozygous mutations in the *DAG1* gene in the described patient

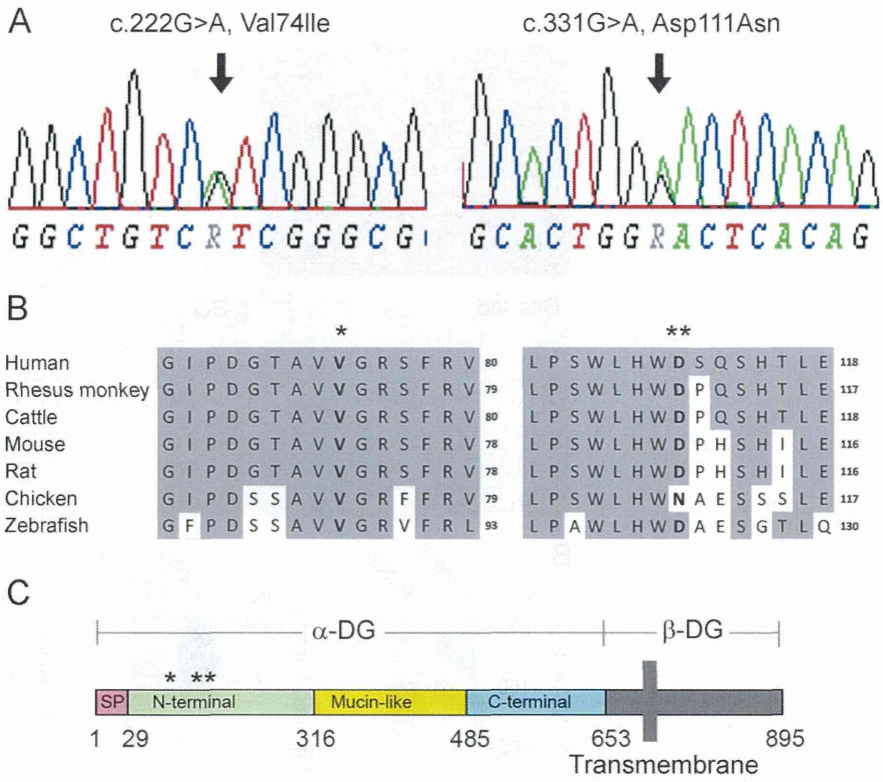

(A) Electropherograms around the mutation sites in *DAG1* genes from Sanger sequencing. (B) Amino acid conservation in mutation sites among species. (C) Localization of mutation sites (* and **) in domain structures in DAG1 protein. DG = dystroglycan.

and 5 months, he became dehydrated in the wake of acute tonsillitis, and was diagnosed with hyperCKemia by chance. After recovery from dehydration, hyperCKemia continued (range, 1,855–6,512 IU/L; normal range, 45–287 IU/L). Physical examination showed no symptomatic muscle weakness but we observed calf pseudohypertrophy. Muscle CT imaging showed low intensity in the rectus femoris, semimembranosus, and gastrocnemius muscles. Brain CT images showed no morphologic abnormality.

Muscle histologic analysis showed muscular dystrophy–like appearance including a few regenerating fibers, internal nuclei, and mild endomysial fibrosis. Immunohistochemical analysis was positive for dystrophin, merosin, sarcoglycans, and β-dystroglycan, but negative for glycoepitope of α-dystroglycan (figure 2). Results of Western blotting and the laminin overlay assay of muscle proteins corroborated the reduction in glycosylation of α-dystroglycan (figure 2); in contrast, we detected strong immunoreactivity to GT20ADG at lower molecular mass. β-Dystroglycan was normal.

Pathogenesis is proven by rescue of *DAG1*-KO HAP1 cells by the wild-type and mutant *DAG1* gene. To prove the pathogenicity of the 2 missense mutations harbored by this patient, we transfected lentivirus vectors with wild-type or mutated DAG1 cDNAs (p.Val74Ile and p.Asp111Asn) into *DAG1*-KO HAP1 cells, which showed defects in reactivity for the anti-α-dystroglycan antibody, IIH6 (figure 3A). *DAG1*-KO HAP1 cells were rescued by introduction of wild-type cDNA showing recovery of strong IIH6 immunoreactivity similar to that of wild-type HAP1 cells (figure 3A). On the contrary, cDNAs with p.Val74Ile and p.Asp111Asn mutations failed to rescue (figure 3A).

We also analyzed mutated β-dystroglycan transport to the cell surface in HAP1 cells. *DAG1*-KO cells were negative for β-dystroglycan staining (figure 3B). Introduction of wild-type and mutated DAG1 cDNAs into *DAG1*-KO cells resulted in recovery of β-dystroglycan staining at the cell surface (in red) but not in the Golgi apparatus (GM130, blue), suggesting that processing and transport of dystroglycan was not affected by the mutations. Cell-surface biotin-labeling experiments in *DAG1*-KO cells transfected with wild-type and mutated DAG1 cDNAs also showed recovery of β-dystroglycan in the biotinylated protein fraction (figure 3C). These results demonstrate that these 2 mutations are pathogenic and impair glycosylation of α-dystroglycan, but not dystroglycan expression.

Figure 2 Hypoglycosylation of α-dystroglycan in the described patient

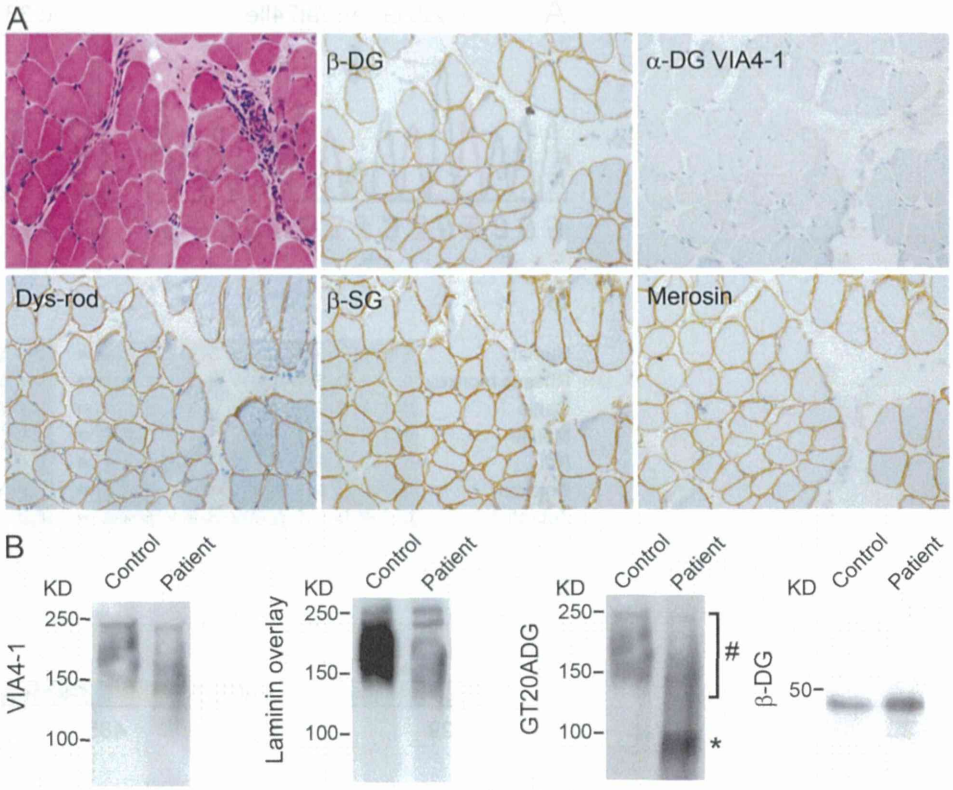

(A, top) Histology and immunostaining of skeletal muscle from the patient. Muscle histology showed muscular dystrophy-like appearance including a few regenerating fibers, internal nuclei, and mild endomysial fibrosis. (A, bottom) Muscle stained positive for antibodies to dystrophin (Dys-rod), merosin, β-sarcoglycan (β-SG), and β-dystroglycan (β-DG), but negative for glycoepitope antibody to α-dystroglycan (α-DG VIA4-1). (B) Western blotting with VIA4-1 antibody and the laminin overlay assay of muscle proteins showing reduced glycosylation of α-dystroglycan; in contrast, strong immunoreactivity to GT20ADG for core peptide was detected at lower molecular mass (*). After Western blotting with VIA4-1 antibody, the same membrane was used for GT20ADG. The bands labeled with # were the VIA4-1 antibody-reactive bands. β-Dystroglycan staining was normal.

DISCUSSION Herein, we report on a patient with dystroglycanopathy, who has compound heterozygous mutations in *DAG1*. This patient had asymptomatic hyperCKemia with mild muscular dystrophy and deficiency in laminin-binding glycosylation in α-dystroglycan. Although the patient could be presymptomatic for muscle weakness or intellectual disability, the clinical phenotype is much milder compared with a previous report of a patient who had limb-girdle–type muscular dystrophy accompanied by mild cognitive impairment.[19] Our finding expands the clinical and pathologic spectrum of dystroglycanopathy associated with *DAG1* mutation from a muscle-eye-brain disease–like phenotype and mild limb-girdle muscular dystrophy[19,20] to asymptomatic hyperCKemia. Myopathic asymptomatic hyperCKemia has been reported in secondary dystroglycanopathies, with mutations in *FKRP* and *FKTN* genes.[24–26] By WES, we also identified 2 missense alterations in each of the *TTN* and *AHNAK* genes, which have been known to be expressed in skeletal muscles. Both alterations in *TTN* were predicted as probably damaging in PolyPhen-2 or disease-causing in MutationTaster in silico functional analyses. These alterations in *TTN* were not localized in the exons in which the mutations have been identified in other muscle diseases, such as hereditary myopathy with early respiratory failure, cardiomyopathy, or tibial muscular dystrophy. *AHNAK* missense alterations were predicted as probably damaging and benign in PolyPhen-2 or polymorphism in MutationTaster. Functional experiments for the mutated proteins would be required for final conclusion of their pathogenicities.

Although one could argue whether the c.220G>A and c.331G>A variants previously annotated in the dbSNP131, 1000 Genomes, and HapMap databases can be the candidate pathogenic mutations, we still presume they are pathogenic because we did not find any other strong candidate gene for dystroglycanopathy in this patient. Because it is known that the 3-kb retrotransposal insertion in *FKTN* with a frequency of 1/88 allele is associated with a high prevalence of Fukuyama congenital muscular dystrophy in Japan,[27]

Figure 3 Mutant *DAG1* observed in patients does not rescue hypoglycosylation of α-dystroglycan in *DAG1*-KO cells

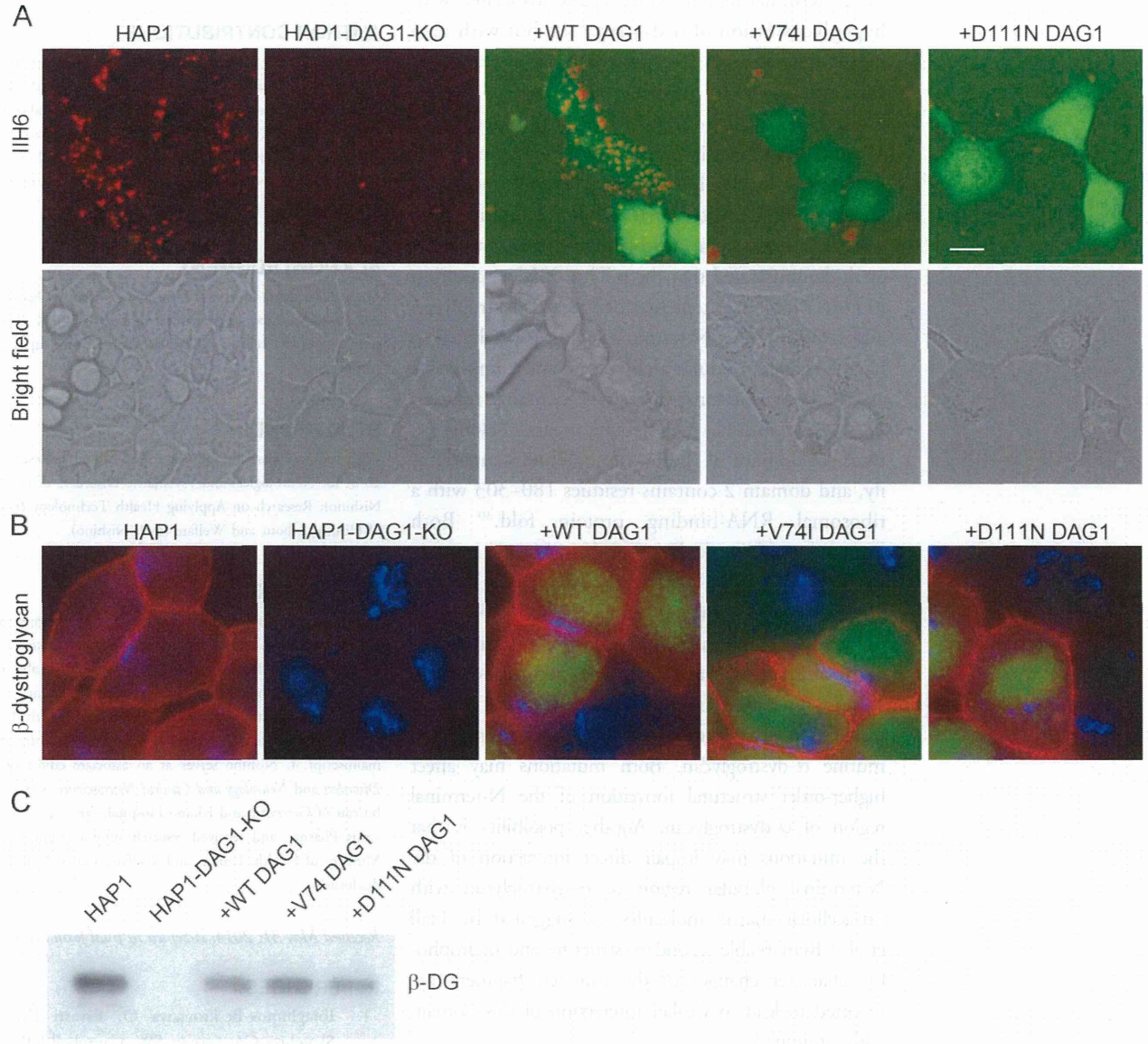

(A) IIH6-4C2 staining of wild-type HAP1 cells (in red), DAG1-knockout cells (HAP1-DAG1-KO), and DAG1-KO cells transfected with wild-type (+WT-DAG1), Val74Ile-mutated (+V74I DAG1), and Asp111Asn-mutated DAG1 (+D111N DAG1). Transfected cells are positive for ZsGreen expression (in green). (B, C) Recovery of β-dystroglycan on cell surface in DAG1-KO cells by transfection with wild-type (+WT-DAG1), p.Val74Ile-mutated (+V74I DAG1), and p.Asp111Asn-mutated DAG1 (+D111N DAG1). HAP1, wild-type haploid cells; HAP1-DAG1-KO, DAG1-KO HAP1 cells. (B) Immunostaining of β-dystroglycan (red) and Golgi protein, GM130 (blue). (C) Western blot analysis of cell-surface biotin-labeled fraction. Scale bar denotes 20 μm. β-DG = β-dystroglycan.

it is logical to suspect a mutation with a variation frequency of more than 0.01. Because the c.331G>A mutation has a variation frequency of 0.005 in all populations in 1000 Genomes and a higher frequency (0.028) in the Japanese population in the Human Genetic Variation Database, there is a possibility that a higher incidence of potential dystroglycanopathy caused by p.Asp111Asn substitution exists in the Japanese population. However, in other populations, the frequency has not been known.

As reported, hypoglycosylation levels of α-dystroglycan do not consistently correlate with clinical severity.[28] Our patient should be classified as having a primary dystroglycanopathy with mutations in *DAG1*; he had typical hypoglycosylation of α-dystroglycan in terms of low molecular mass of the protein, positive reactivity to anti-core peptide antibody, and decreased binding to laminin, but he showed a milder phenotype. The level of hypoglycosylation of α-dystroglycan is not necessarily predictive of phenotypic severity in dystroglycanopathy.

Our results suggest that the missense mutation of p.Val74Ile or p.Asp111Asn in the N-terminal region of α-dystroglycan does not influence expression of the dystroglycan, but it does cause a defect in

posttranslational modification. Similarly, Hara et al.[19] reported a missense mutation (p.The192Met) in the N-terminal region, which is also associated with hypoglycosylation of α-dystroglycan but with normal β-dystroglycan localization. LARGE catalyzes the extension of specific disaccharide structures [−3GlcAα1−4Xylβ1−] on a phosphorylated *O*-mannosyl glycan in the mucin-like domain, which is required for laminin binding, within the Golgi apparatus.[29] The N-terminal region in α-dystroglycan serves as a recognition site for LARGE[8]; of note, Hara et al. demonstrated that the p.The192Met mutation in *DAG1* impairs interaction between α-dystroglycan and LARGE. This N-terminal region is predicted to have L-shaped modular architecture and comprises 2 autonomous domains; domain 1 contains residues 28–168 in murine α-dystroglycan and belongs to the I-set domain of the immunoglobulin superfamily, and domain 2 contains residues 180–303 with a ribosomal RNA-binding protein fold.[30] Both mutated residues, Val74 and Asp111, are present in domain 1 and are neighbors of Gly75 and Gln113 (corresponding to Gly73 and His111in murine dystroglycan); each of these is predicted to be aligned on the interaction between domain 1 and 2, and the trimer interface of domain 1, respectively, in the crystal structure of the N-terminal region of murine α-dystroglycan. Both mutations may affect higher-order structural formation of the N-terminal region of α-dystroglycan. Another possibility is that the mutations may impair direct interaction of the N-terminal globular region of α-dystroglycan with extracellular matrix molecules, as suggested by Hall et al.[31] Remarkable secondary structure and hydrophobic character changes of the mutated fragment are reported to lead to weaker interaction of this domain with laminin.[32]

Previously, Willer et al.[15] have demonstrated the rescuing experiments using patients' fibroblasts in dystroglycanopathy for evaluation of the pathogenicity of gene mutations. In this study, we used gene-modified HAP1 cells because the patient's cells were not available. The phenotypic rescue experiments described here, using *DAG1*-KO HAP1 cells with lentivirus-mediated expression of mutated cDNA, enabled rapid and easy evaluation of the pathogenicity of the mutations. This is a simple method based on the recovery of the function of α-dystroglycan. Theoretically, this method can be applied to evaluate any of the mutations in all known causative genes as well as mutations in novel candidate genes for dystroglycanopathies without requiring enzymatic activity measurement, as long as the specific gene-KO HAP1 cells are available. This method would be applicable by any researcher for confirming the data from WES for each causative mutation in any disease, if the phenotypes of cells were characterized.

AUTHOR CONTRIBUTIONS

M.D. conducted acquisition, analysis and interpretation of data, and drafted and edited the manuscript. S.N. supervised all aspects of this study including study design, data interpretation, and drafted and edited the manuscript. Y.E. made WES pipeline and analyzed the data. Y.K.H. selected patients and performed WES. S.Y. collected clinical information of the patient. I. Nonaka and I. Nishino supervised manuscript preparation and edited the manuscript.

ACKNOWLEDGMENT

The authors thank Nozomi Matsuyama, Megumu Ogawa, Kanako Goto, and Asako Kaminaga for technical support, Thijn R. Brummelkamp for supplying HAP1 cells, and Kevin P. Campbell for supplying GT20ADG antibody.

STUDY FUNDING

This study was partially supported by Intramural Research Grant (25-5, 26-8) for Neurological and Psychiatric Disorders of NCNP (to S.N., I. Nishino); Research on Applying Health Technology from the Ministry of Health, Labour and Welfare (to I. Nishino).

DISCLOSURE

M. Dong reports no disclosures relevant to the manuscript. S. Noguchi serves as an editor of *Acta Neuropathologica Communications* and received research support from the Ministry of Health, Labour and Welfare. Y. Endo reports no disclosures relevant to the manuscript. Y. Hayashi received research support from the Ministry of Health, Labour and Welfare. S. Yoshida and I. Nonaka report no disclosures relevant to the manuscript. I. Nishino serves as an associate editor of *Neuromuscular Disorders* and *Neurology and Clinical Neuroscience*, serves on the speakers bureau of Genzyme and Kitano Hospital, serves as a consultant of Novartis Pharma, and received research support from Genzyme and the Ministry of Health, Labour and Welfare. Go to Neurology.org for full disclosures.

Received May 31, 2014. Accepted in final form September 29, 2014.

REFERENCES

1. Ibraghimov-Beskrovnaya O, Ervasti JM, Leveille CJ, Slaughter CA, Sernett SW, Campbell KP. Primary structure of dystrophin-associated glycoproteins linking dystrophin to the extracellular matrix. Nature 1992;355:696–702.
2. Michele DE, Barresi R, Kanagawa M, et al. Post-translational disruption of dystroglycan-ligand interactions in congenital muscular dystrophies. Nature 2002;418:417–422.
3. Moore SA, Saito F, Chen J, et al. Deletion of brain dystroglycan recapitulates aspects of congenital muscular dystrophy. Nature 2002;418:422–425.
4. Saito F, Moore SA, Barresi R, et al. Unique role of dystroglycan in peripheral nerve myelination, nodal structure, and sodium channel stabilization. Neuron 2003;38:747–758.
5. Durbeej M, Talts JF, Henry MD, Yurchenco PD, Campbell KP, Ekblom P. Dystroglycan binding to laminin alpha1LG4 module influences epithelial morphogenesis of salivary gland and lung in vitro. Differentiation 2001;69:121–134.
6. Matsumura K, Chiba A, Yamada H, et al. A role of dystroglycan in schwannoma cell adhesion to laminin. J Biol Chem 1997;272:13904–13910.

7. Noguchi S, Wakabayashi E, Imamura M, Yoshida M, Ozawa E. Formation of sarcoglycan complex with differentiation in cultured myocyte. Eur J Biochem 2000;267: 640–648.
8. Kanagawa M, Saito F, Kunz S, et al. Molecular recognition by LARGE is essential for expression of functional dystroglycan. Cell 2004;117:953–964.
9. Brancaccio A, Schulthess T, Gesemann M, Engel J. Electron microscopic evidence for a mucin-like region in chick muscle alpha-dystroglycan. FEBS Lett 1995;368: 139–142.
10. Chiba A, Matsumura K, Yamada H, et al. Structures of sialylated O-linked oligosaccharides of bovine peripheral nerve alpha-dystroglycan: the role of a novel O-mannosyl-type oligosaccharide in the binding of alpha-dystroglycan with laminin. J Biol Chem 1997; 272:2156–2162.
11. Hara Y, Kanagawa M, Kunz S, et al. Like-acetylglucosaminyltransferase (LARGE)-dependent modification of dystroglycan at Thr-317/319 is required for laminin binding and arenavirus infection. Proc Natl Acad Sci USA 2011;108:17426–17431.
12. Muntoni F, Brockington M, Brown SC. Glycosylation eases muscular dystrophy. Nat Med 2004;10:676–677.
13. Brown SC, Torelli S, Brockington M. Abnormalities in alpha-dystroglycan expression in MDC1C and LGMD2I muscular dystrophies. Am J Pathol 2004;164:727–737.
14. Mendell JR, Boué DR, Martin PT. The congenital muscular dystrophies: recent advances and molecular insights. Pediatr Dev Pathol 2006;9:427–443.
15. Willer T, Lee H, Lommel M, et al. ISPD loss-of-function mutations disrupt dystroglycan O-mannosylation and cause Walker-Warburg syndrome. Nat Genet 2012;44: 575–580.
16. Roscioli T, Kamsteeg EJ, Buysse K, et al. Mutations in ISPD cause Walker-Warburg syndrome and defective glycosylation of α-dystroglycan. Nat Genet 2012;44: 581–585.
17. Manzini MC, Tambunan DE, Hill RS, et al. Exome sequencing and functional validation in zebrafish identify GTDC2 mutations as a cause of Walker-Warburg syndrome. Am J Hum Genet 2012;91:541–547.
18. Carss KJ, Stevens E, Foley AR, et al. Mutations in GDP-mannose pyrophosphorylase B cause congenital and limb-girdle muscular dystrophies associated with hypoglycosylation of α-dystroglycan. Am J Hum Genet 2013; 93:29–41.
19. Hara Y, Balci-Hayta B, Yoshida-Moriguchi T, et al. A dystroglycan mutation associated with limb-girdle muscular dystrophy. N Engl J Med 2011;364:939–946.
20. Geis T, Marquard K, Rödl T. Homozygous dystroglycan mutation associated with a novel muscle-eye-brain disease-like phenotype with multicystic leucodystrophy. Neurogenetics 2013;14:205–213.
21. Hayashi YK, Ogawa M, Tagawa K, et al. Selective deficiency of alpha-dystroglycan in Fukuyama-type congenital muscular dystrophy. Neurology 2001;57:115–121.
22. Saitsu H, Nishimura T, Muramatsu K, et al. De novo mutations in the autophagy gene WDR45 cause static encephalopathy of childhood with neurodegeneration in adulthood. Nat Genet 2013;45:445–449.
23. Jae LT, Raaben M, Riemersma M, et al. Deciphering the glycosylome of dystroglycanopathies using haploid screens for lassa virus entry. Science 2013;340:479–483.
24. de Paula F, Vieira N, Starling A, et al. Asymptomatic carriers for homozygous novel mutations in the FKRP gene: the other end of the spectrum. Eur J Hum Genet 2003;11:923–930.
25. Fernandez C, de Paula AM, Figarella-Branger D, et al. Diagnostic evaluation of clinically normal subjects with chronic hyperCKemia. Neurology 2006;66:1585–1587.
26. Fiorillo C, Moro F, Astrea G, et al. Novel mutations in the fukutin gene in a boy with asymptomatic hyperCKemia. Neuromuscul Disord 2013;23:1010–1015.
27. Colombo R, Bignamini AA, Carobene A, et al. Age and origin of the FCMD 3'-untranslated-region retrotransposal insertion mutation causing Fukuyama-type congenital muscular dystrophy in the Japanese population. Hum Genet 2000;107:559–567.
28. Jimenez-Mallebrera C, Torelli S, Feng L, et al. A comparative study of alpha-dystroglycan glycosylation in dystroglycanopathies suggests that the hypoglycosylation of alpha-dystroglycan does not consistently correlate with clinical severity. Brain Pathol 2009;19:596–611.
29. Yoshida-Moriguchi T, Yu L, Stalnaker SH, et al. O-mannosyl phosphorylation of alpha-dystroglycan is required for laminin binding. Science 2010;327:88–92.
30. Bozic D, Sciandra F, Lamba D, Brancaccio A. The structure of the N-terminal region of murine skeletal muscle alpha-dystroglycan discloses a modular architecture. J Biol Chem 2004;279:44812–44816.
31. Hall H, Bozic D, Michel K, Hubbell JA. N-terminal alpha-dystroglycan binds to different extracellular matrix molecules expressed in regenerating peripheral nerves in a protein-mediated manner and promotes neurite extension of PC12 cells. Mol Cell Neurosci 2003;24:1062–1073.
32. Bhattacharya S, Das A, Ghosh S, Dasgupta R, Bagchi A. Hypoglycosylation of dystroglycan due to T192M mutation: a molecular insight behind the fact. Gene 2014;537: 108–114.

RESEARCH PAPER

Mutation profile of the *GNE* gene in Japanese patients with distal myopathy with rimmed vacuoles (GNE myopathy)

Anna Cho,[1] Yukiko K Hayashi,[1,2,3] Kazunari Monma,[1] Yasushi Oya,[4] Satoru Noguchi,[1] Ikuya Nonaka,[1] Ichizo Nishino[1,2]

ABSTRACT

Background GNE myopathy (also called distal myopathy with rimmed vacuoles or hereditary inclusion body myopathy) is an autosomal recessive myopathy characterised by skeletal muscle atrophy and weakness that preferentially involve the distal muscles. It is caused by mutations in the gene encoding a key enzyme in sialic acid biosynthesis, UDP-*N*-acetylglucosamine 2-epimerase/*N*-acetylmannosamine kinase (GNE).

Methods We analysed the *GNE* gene in 212 Japanese GNE myopathy patients. A retrospective medical record review was carried out to explore genotype–phenotype correlation.

Results Sixty-three different mutations including 25 novel mutations were identified: 50 missense mutations, 2 nonsense mutations, 1 insertion, 4 deletions, 5 intronic mutations and 1 single exon deletion. The most frequent mutation in the Japanese population is c.1714G>C (p.Val572Leu), which accounts for 48.3% of total alleles. Homozygosity for this mutation results in more severe phenotypes with earlier onset and faster progression of the disease. In contrast, the second most common mutation, c.527A>T (p.Asp176Val), seems to be a mild mutation as the onset of the disease is much later in the compound heterozygotes with this mutation and c.1714G>C than the patients homozygous for c.1714G>C. Although the allele frequency is 22.4%, there are only three homozygotes for c.527A>T, raising a possibility that a significant number of c.527A>T homozygotes may not develop an apparent disease.

Conclusions Here, we report the mutation profile of the *GNE* gene in 212 Japanese GNE myopathy patients, which is the largest single-ethnic cohort for this ultra-orphan disease. We confirmed the clinical difference between mutation groups. However, we should note that the statistical summary cannot predict clinical course of every patient.

INTRODUCTION

GNE myopathy, which is also known as distal myopathy with rimmed vacuoles,[1] quadriceps sparing myopathy[2] or hereditary inclusion body myopathy (hIBM),[3] is an autosomal recessive myopathy characterised by skeletal muscle atrophy and weakness that preferentially involve the distal muscles such as the tibialis anterior. It is a progressive disease, whereby the symptoms of muscle weakness start to affect the patient from the second or third decade of life, and most of the patients become wheelchair-bound between twenties and sixties.[4] The characteristic histopathological features in muscle biopsy include muscle fibre atrophy with the presence of rimmed vacuoles and intracellular congophilic deposits.[4 5] GNE myopathy is caused by mutations in the gene encoding a key enzyme in sialic acid biosynthesis, UDP-*N*-acetylglucosamine 2-epimerase/*N*-acetylmannosamine kinase (GNE).[6–8] Genetically confirmed GNE myopathy was initially recognised in Iranian Jews and Japanese,[7 9] but later appeared to be widely distributed throughout the world. More than 100 mutations in the *GNE* gene have been described up to date.

During the last decade, there has been extensive experimental work to elucidate the pathogenesis and to develop therapeutic strategies of GNE myopathy.[6 10–12] Better knowledge on the basis of those research achievements have currently enabled us to enter the era of clinical trial for human patients. At this moment, the identification of new GNE myopathy patients with precise genetic diagnosis and the expansion of global spectrum of *GNE* mutations are timely and important. Here, we report the molecular profile of Japanese GNE myopathy patients with a brief discussion of genotype–phenotype correlations.

METHODS

Patients

Two hundred and twelve patients from 201 unrelated Japanese families were included in this study. There were 117 female and 95 male patients. All cases were genetically confirmed as GNE myopathy. A retrospective medical record review was carried out to explore genotype–phenotype correlation. Informed consent was obtained for the collection of clinical data and extraction of DNA to perform mutation analysis.

Genetic analysis

DNA was extracted from peripheral blood leukocytes or skeletal muscle tissue. We used the previously described sequencing method to describe mutations at cDNA level.[7] All exons and splice regions of the *GNE* gene were sequenced. NM_005476.5 was used as a reference sequence. We screened 100 alleles from normal Japanese individuals to determine the significance of novel variations.

Pathological analysis

To evaluate histopathological phenotype according to genotype, we analysed muscle biopsies from two

▶ Additional material is published online only. To view please visit the journal online (http://dx.doi.org/10.1136/jnnp-2013-305587).

[1]Department of Neuromuscular Research, National Institute of Neuroscience, National Center of Neurology and Psychiatry, Tokyo, Japan
[2]Department of Clinical Development, Translational Medical Center, National Center of Neurology and Psychiatry, Tokyo, Japan
[3]Department of Neurophysiology, Tokyo Medical University, Tokyo, Japan
[4]Department of Neurology, National Center Hospital, National Center of Neurology and Psychiatry, Tokyo, Japan

Correspondence to
Professor Yukiko K Hayashi, Department of Neurophysiology, Tokyo Medical University, 6-1-1 Shinjuku, Shinjuku, Tokyo 160-8402, Japan; yhayashi@tokyo-med.ac.jp

Received 4 June 2013
Revised 21 August 2013
Accepted 22 August 2013
Published Online First 11 September 2013

▶ http://dx.doi.org/10.1136/jnnp-2013-306414

To cite: Cho A, Hayashi YK, Monma K, *et al*. *J Neurol Neurosurg Psychiatry* 2014;**85**:912–915.